



Novel *KAT6B::NUTM2B* fusion oncogene in congenital acute myeloid leukemia and implications for menin inhibitor therapy

by Rebecca K. Voss, Wenqing Qi, La'Ron Browne, Ruth W. Wang'ondou, Mahsa Khanlari, Jing Ma, Xuefei Ma, Josi Lott, Juan M. Barajas, Melvin Thomas III, Victor B Pastor Loyola, Hui Cao, Larissa V. Furtado, Swati Naik, Sakshi Bami, Seth E. Karol, Jeffrey E. Rubnitz, Jeffery M. Klco, Yen-Chun Liu and Lu Wang

Received: December 10, 2025.

Accepted: April 10, 2026.

Citation: Rebecca K. Voss, Wenqing Qi, La'Ron Browne, Ruth W. Wang'ondou, Mahsa Khanlari, Jing Ma, Xuefei Ma, Josi Lott, Juan M. Barajas, Melvin Thomas III, Victor B Pastor Loyola, Hui Cao, Larissa V. Furtado, Swati Naik, Sakshi Bami, Seth E. Karol, Jeffrey E. Rubnitz, Jeffery M. Klco, Yen-Chun Liu and Lu Wang. Novel *KAT6B::NUTM2B* fusion oncogene in congenital acute myeloid leukemia and implications for menin inhibitor therapy. *Haematologica*. 2026 Apr 23. doi: 10.3324/haematol.2025.300350 [Epub ahead of print]

Publisher's Disclaimer.

E-publishing ahead of print is increasingly important for the rapid dissemination of science.

Haematologica is, therefore, E-publishing PDF files of an early version of manuscripts that have completed a regular peer review and have been accepted for publication.

E-publishing of this PDF file has been approved by the authors.

After having E-published Ahead of Print, manuscripts will then undergo technical and English editing, typesetting, proof correction and be presented for the authors' final approval; the final version of the manuscript will then appear in a regular issue of the journal.

All legal disclaimers that apply to the journal also pertain to this production process.

Novel *KAT6B::NUTM2B* fusion oncogene in congenital acute myeloid leukemia and implications for menin inhibitor therapy

Rebecca K. Voss¹, Wenqing Qi¹, La'Ron Browne², Ruth W. Wang'ondu², Mahsa Khanlari¹, Jing Ma¹, Xuefei Ma^{1,3}, Josi Lott⁴, Juan M. Barajas¹, Melvin Thomas III¹, Victor B Pastor Loyola¹, Hui Cao¹, Larissa V. Furtado¹, Swati Naik⁵, Sakshi Bami⁶, Seth E. Karol², Jeffrey E. Rubnitz², Jeffery M. Klco¹, Yen-Chun Liu^{1#}, and Lu Wang^{1#}

1. Department of Pathology, St. Jude Children's Research Hospital, Memphis, TN
2. Department of Oncology, St. Jude Children's Research Hospital, Memphis, TN
3. Department of Laboratory Medicine, Ruijin Hospital, Shanghai Jiao Tong University School of Medicine, Shanghai, China
4. Center of Excellence in Leukemia Studies, St. Jude Children's Research Hospital, Memphis, TN
5. Department of Bone Marrow Transplant and Cellular Therapy, St. Jude Children's Research Hospital, Memphis, TN
6. Department of Hematology/Oncology, St Jude Affiliate Clinic, Our Lady of the Lake Children's Hospital, Baton Rouge, LA

Co-corresponding author

Running head: Congenital AML with *KAT6B::NUTM2B* fusion

Correspondence and requests for materials should be addressed to:

Lu Wang, M.D., Ph.D.
Associate Member, Department of Pathology
St. Jude Children's Research Hospital
262 Danny Thomas Place, Memphis, TN 38105, USA
Email: Lu.Wang2@stjude.org
Tel: 901-595-1163

Yen-Chun Liu, M.D., Ph.D.
Associate Member, Department of Pathology
St. Jude Children's Research Hospital
262 Danny Thomas Place, Memphis, TN 38105, USA
Email: Yen-Chun.Liu@stjude.org
Tel: 901-595-7116

Author contributions

LW, Y-CL and JMK designed the study. LW and Y-CL supervised the conduction of the project. LB, JER, RWW, MK, SN, SB, Y-CL, LW, LVF and SEK contributed to patient care. Y-CL provided morphology and flow cytometry analyses of patient's samples. VBP analyzed patient WGS and WTS data. JM conducted transcriptomic profiling of patients' samples. RKV, WQ, XM and JL conducted in vitro studies. JMB, MTIII and HC provided material and expertise for conducting in vitro studies. RKV generated tables and figures for the manuscript. RKV and LW wrote the manuscript. All authors reviewed and edited the manuscript.

Disclosure of conflicts of interest:

The authors declare no competing financial interests in relation to the work described.

Acknowledgment

We thank Paula Perez-Sanchez at SJCRH Center of Excellence for Leukemia Studies Flow Cytometry Core; Maria Cardenas in Department of Computation Biology for providing *HOXA9/10* expression data of leukemia samples from St. Jude Cloud. We sincerely thank Dr. Yiping Fan from Center for Applied Bioinformatics at SJRCH for his invaluable assistance with RNA-seq data analysis. We thank the staff of SJCRH Flow Cytometry and Cell Sorting Shared Resource (FCCSSR) supported in part by ALSAC and the National Cancer Institute grant P30 CA021765.

Funding: The work was funded by the American Lebanese and Syrian Associated Charities (ALSAC) of St. Jude Children's Research Hospital (SJCRH).

Data sharing: Data are available on request from corresponding authors Dr. Lu Wang (Lu.wang2@stjude.org) and Dr. Yen-Chun Liu (Yen-Chun.Liu@stjude.org)

Word count: Main text (= introduction + methods + results + discussion) = 1484 words;

Three main figures are present in the manuscript;

Supplementary file: One PDF file consists of two supplementary figures and one supplementary table.

Congenital acute myeloid leukemia (AML) is rare and may initially present as myeloid sarcoma. The most common non-Down syndrome related congenital leukemia is AML, with over half involving *KMT2A* or *KAT6A* fusions^{1,2}. *KMT2A*-rearranged infant AML has a poor prognosis, while some cases with *KAT6A* fusions may spontaneously remit². Molecular pathogenesis studies have revealed a functional connection between *KMT2A* and *KAT6A* in transcriptional activation. Both *KMT2A* and *KAT6A* fusion proteins drive aberrant transcription and self-renewal in hematopoietic progenitors, notably activating *HOXA* genes^{3,4}. Inhibitors targeting the *KMT2A/KAT6A* transcriptional complex, especially menin inhibitors, have shown therapeutic promise^{5,6}. Here, we report the identification of a novel *KAT6B::NUTM2B* fusion, involving the *KAT6A* paralog *KAT6B*, in congenital AML and demonstrate its oncogenic activity and sensitivity to menin inhibition through in vitro study in mouse hematopoietic stem and progenitor cells (mHSPCs). Informed consent for clinical genomics testing was obtained from the patient's legal guardians, and this study was approved by the Institutional Review Board (IRB) at St. Jude Children's Research Hospital (SJCRH). The findings expand the knowledge of *KAT6A/B*-rearranged AML and suggest menin inhibitors as a potential therapy.

The patient presented with blueberry muffin rash at birth. A biopsy of the rash revealed myeloid sarcoma. A bone marrow sample collected at day nine after birth showed 37% blasts, positive for MPO and NSE (Figure 1A), and flow cytometry indicated AML with monocytic differentiation (CD11c, CD64, CD33, HLA-DR, CD123, MPO positive; CD14 loss in most blasts; negative for CD34, CD117, CD133, NG2, CD19, CD3) (Supplementary Figure S1A). No clonal abnormalities or *KMT2A* rearrangement were detected by karyotype or FISH. Bone marrow aspirate (BMA) and skin lesion biopsy samples were collected for molecular diagnosis in CLIA-certified laboratory at SJCRH. The fresh BMA sample was subjected to DNA and RNA extraction followed by Clinical Genomics Testing as previously described⁷, including whole genome sequencing (WGS) and whole transcriptome sequencing (WTS). The FFPE tissue of skin lesion biopsy was subjected to

RNA extraction and WTS only. Integrated WGS and WTS analyses identified a cryptic deletion at chromosome region 10q22 resulting in an in-frame *KAT6B::NUTM2B* fusion, preserving the exons encoding the histone acetyltransferase domain of *KAT6B* and most of the coding sequence of *NUTM2B* (Figure 1B). This fusion was the only tumor-acquired likely pathogenic alteration identified and was also detected in the skin rash by WTS. Transcriptomic profiling clustered the case with *KAT6A*- and *KMT2A*-rearranged AML (Figure 1C) and high expression of *HOXA9* and *HOXA10* was observed (Figure 1D). Initial watch-and-wait management was chosen due to possible spontaneous remission¹. At 4 months of age, disease progressed (44% blasts in bone marrow, hemophagocytosis), prompting standard pediatric induction chemotherapy (Supplementary Figure S1B) and subsequent haploidentical stem cell transplant. Full donor engraftment and MRD-negative marrow by flow cytometry was achieved and sustained for several months post-transplant. Relapse occurred at one year (77.6% blasts, testicular myeloid sarcoma), unfortunately, the patient died at 16 months despite further chemotherapy.

To our knowledge, this patient represents the first reported case in an infant and the fifth case of a myeloid malignancy harboring a *KAT6B* gene fusion, as well as the first reported instance of a *KAT6B::NUTM2B* fusion. The four previously reported cases all carried a *KAT6B::CREBBP* fusion, which is considered a variant of *KAT6A::CREBBP* (Supplementary Table S1). *KAT6A::CREBBP* is a rare but recurrent AML-defining fusion⁸, with other *KAT6A* fusion partners (*NCOA2*, *NCOA3*, *EP300*, *LEUTX*, *ASXL2*) also reported in myeloid malignancies (Supplementary Table S1). Review of infant AML with *KAT6A* fusions shows that over 80% of patients presented with skin lesions (myeloid sarcoma). Bone marrow involvement typically showed morphological features consistent with AML FAB subtype M4 or M5, with erythrophagocytosis observed in up to 50% of cases. Hepatosplenomegaly was frequently present, and up to 30% of patients showed disseminated intravascular coagulation. Spontaneous remission occurred in up to 45% of congenital AML patients with *KAT6A*-rearrangement. Overall, the current case with a novel *KAT6B::NUTM2B* fusion shares clinical features similar to those

observed in infant AML with *KAT6A* fusions; however, despite remaining clinically stable with improvement of skin lesions for approximately 4 months without treatment, the patient ultimately had a poor clinical outcome.

To gain deeper insights into the novel *KAT6B::NUTM2B* fusion, the full-length coding sequence of *KAT6B::NUTM2B* fusion as well as controls (wild-type *KAT6B* and *NUTM2B*) were cloned into MSCV-IRES-GFP (MPG) lentiviral expression vector, respectively, and transduced into C57BL/6J murine bone marrow hematopoietic stem and progenitor cells (mHSPC) to assess the transforming properties of *KAT6B::NUTM2B*. Initially, *Hoxa9* and *Hoxa10* mRNA were assessed in mHSPCs expressing either wild-type *KAT6B* (*KAT6B*-mHSPC) or *KAT6B::NUTM2B* (*KN*-mHSPC). Consistent with elevated *HOXA9/10* expression observed in the patient's leukemia sample, there was a significant upregulation of *Hoxa9* and *Hoxa10* in *KN*-mHSPCs (Supplementary figure S2B). The mHSPCs transduced with *KAT6B::NUTM2B* or controls were plated in semi-solid methylcellulose-based media for colony forming unit (CFU) assay. Colonies were counted, harvested, and serially replated every 7 days (Figure 2A, I). The *KN*-mHSPCs exhibited a significant and sustained increase in colony formation, with successful serial replating for 4 weeks or longer, in contrast to wild-type *KAT6B* or *NUTM2B*, or empty vector controls (Figure 2B). Considering the *HOXA9/10* activation in the patient's leukemia, *KN*-mHSPCs were treated with SNDX-5613, a clinical-grade menin inhibitor, at three different concentrations over a three-week period (Figure 2A, II and III). We evaluated the sensitivity of *KAT6B::NUTM2B* fusion to SNDX-5613 in comparison with two common fusions in pediatric AML: *RUNX1::RUNX1T1* (9a isoform⁹) serving as a negative control as it is not considered a primary target of menin inhibitors, and *NUP98::KDM5A*, which is associated with *HOXA* activation and sensitivity to menin inhibitors¹⁰, serving as a positive control. An empty vector control was also included. By the end of week three, colony formation of *KN*-mHSPCs was reduced by approximately 90-95% with SNDX-5613 treatment at all three concentrations, *NUP98::KDM5A*-transduced cells also exhibited a dose-dependent reduction in colony formation with SNDX-5613, albeit less

prominently than *KN*-mHSPCs. In contrast, no significant change was seen in controls (empty vector or *RUNX1::RUNX1T1*-transduced cells) (Figure 2C). Besides the reduction of clonogenic growth, SNDX-5613 treatment resulted in a significant increase in Gr1 and CD11b positivity and a concomitant decrease in CD117 (cKIT) expression in both *KAT6B::NUTM2B* and *NUP98::KDM5A* transduced mHSPCs, indicating myeloid maturation and loss of stemness (Figure 2D). Additionally, menin inhibition resulted in significantly reduced *Hoxa9/10* mRNA expression (Figure 2E) and morphological changes in *KN*-mHSPCs (Figure 2F).

Both *KAT6A* and *KAT6B* encode histone acetyltransferases (HAT) that are core components of the MOZ/MORF complex¹¹ and closely interact with the KMT2A (a.k.a. MLL) complex, facilitating histone acetylation and cooperatively promoting transcription of genes regulating hematopoiesis³. While wild-type *KAT6A* and *KAT6A* fusions have been functionally characterized, the role of *KAT6B* in hematopoiesis has only recently been recognized¹². Fusions involving *KAT6A* or *KAT6B* retain 5' exons encoding the MYST (histone acetyltransferase) domain (Figure 3), thereby preserving N-terminal functional domains of *KAT6A/B* in the resulting chimeric proteins. Notably, nearly all previously reported fusion partners of *KAT6A/B* are transcriptional co-activators (such as *CREBBP*, *EP300*, *NCOA2*, *NCOA3*) or are predicted to possess a transcriptional activation domain (e.g. *LEUTX*), with these activation domains consistently retained as C-terminal regions in the fusion proteins. Consequently, *KAT6A/B* fusions typically contain one or more HAT domains capable of modifying chromatin and activating genes such as the *HOXA* cluster. While *NUTM2B* has been reported in *YWHAE::NUTM2B* fusion in sarcomas, the function of wild-type *NUTM2B* is unclear. Interestingly, a recent study reported that *YWHAE::NUTM2B* can interact with *EP300* and *CREBBP*¹³. Although the specific functional domain mediating the interaction with *EP300/CREBBP* was not elucidated in the study of *YWHAE::NUTM2B*, it raises the possibility that *KAT6B::NUTM2B* may similarly recruit these co-activators to promote the transcription of *HOXA* genes, akin to *KAT6A/B::NCOA2* fusions.

Previous studies have shown that the *KAT6A::NCOA2* fusion protein targets chromatin in a wild-type KMT2A-dependent manner³. Menin plays a central role by tethering the KMT2A complex to DNA⁶ and recruiting *KAT6A/B*-fusion proteins³. Menin inhibitors have demonstrated therapeutic efficacy in *KMT2A-r* AML¹⁴, and emerging evidence from other *HOXA*-activating AMLs, including *KAT6A-r*³ and *NUP98-r* AML¹⁰, suggests a similar vulnerability. Consistent with this model, treating *KN*-mHSPCs with menin inhibitor SNDX-5613 impaired colony formation, promoted myeloid differentiation, and reduced *Hoxa9/10* expression, supporting menin dependency in *KAT6B::NUTM2B* leukemogenesis. Our findings align with a previous study on *KAT6A::NCOA2*¹¹ and further indicate that menin inhibition may hold therapeutic potential against *KAT6A/B-r* AML.

In this study, we report a novel *KAT6B::NUTM2B* fusion in a congenital AML patient whose clinical and transcriptomic features resembled those of *KAT6A::CREBBP*-positive infant AML, indicating a shared mechanism. *KAT6B::NUTM2B* fusion drove oncogenic transformation in vitro, and *KN*-mHSPCs were vulnerable to menin inhibitor, supporting therapeutic potential of menin inhibition for *KAT6B-r* AML. Further studies utilizing primary leukemia samples from AML patients harboring *KAT6A/B*-fusions are required to validate these findings. Given the increasing recognition of resistance to menin inhibitors¹⁵, alternative therapeutic strategies, such as *KAT6* inhibitors or combination therapies, should be investigated. Overall, our findings provide critical new insights into the biology of *KAT6B* fusions and nominate a therapeutic strategy for this rare leukemia.

References

1. Calvo C, Fenneteau O, Leverger G, Petit A, Baruchel A, Mechinaud F. Infant Acute Myeloid Leukemia: A Unique Clinical and Biological Entity. *Cancers (Basel)*. 2021;13(4):777.
2. Coenen EA, Zwaan CM, Reinhardt D, et al. Pediatric acute myeloid leukemia with t(8;16)(p11;p13), a distinct clinical and biological entity: a collaborative study by the International-Berlin-Frankfurt-Munster AML-study group. *Blood*. 2013;122(15):2704-2713.
3. Miyamoto R, Okuda H, Kanai A, et al. Activation of CpG-Rich Promoters Mediated by MLL Drives MOZ-Rearranged Leukemia. *Cell Rep*. 2020;32(13):108200.
4. Paggetti J, Largeot A, Aucagne R, et al. Crosstalk between leukemia-associated proteins MOZ and MLL regulates HOX gene expression in human cord blood CD34+ cells. *Oncogene*. 2010;29(36):5019-5031.
5. White J, Derheimer FA, Jensen-Pergakes K, et al. Histone lysine acetyltransferase inhibitors: an emerging class of drugs for cancer therapy. *Trends Pharmacol Sci*. 2024;45(3):243-254.
6. Schurer A, Glushakow-Smith SG, Gritsman K. Targeting chromatin modifying complexes in acute myeloid leukemia. *Stem Cells Transl Med*. 2025;14(2):szae089.
7. Voss RK, Pastor Loyola VB, Cardenas MF, et al. Clinical experience of using integrated whole genome and transcriptome sequencing as a framework for pediatric and adolescent acute myeloid leukemia diagnosis and risk assessment. *Leukemia*. 2025;39(12):2946-2956.
8. Li W. The 5th Edition of the World Health Organization Classification of Hematolymphoid Tumors. In: Li W, ed. *Leukemia [Internet]*. Brisbane (AU): Exon Publications, 2022. Chapter 1.
9. Thomas MIII, Qi WQ, Walsh MP, et al. Functional characterization of cooperating mutations in acute myeloid leukemia. *Leukemia*. 2024;38(5):991-1002.
10. Michmerhuizen NL, Heikamp EB, Iacobucci I, et al. KAT6A and KAT7 Histone Acetyltransferase Complexes Are Molecular Dependencies and Therapeutic Targets in NUP98 -Rearranged Acute Myeloid Leukemia. *Cancer Discov*. 2025;15(10):2096-2116.

11. Ullah M, Pelletier N, Xiao L, et al. Molecular architecture of quartet MOZ/MORF histone acetyltransferase complexes. *Mol Cell Biol*. 2008;28(22):6828-6843.
12. Bergamasco MI, Ranathunga N, Abeysekera W, et al. The histone acetyltransferase KAT6B is required for hematopoietic stem cell development and function. *Stem Cell Reports*. 2024;19(4):469-485.
13. Brahmi M, Duc A, Vanacker H, et al. P435) Oncogenic Fusion YWHAE::NUTM2 Disrupt EP300/BCOR Interaction.
<https://ctos2023.eventscribe.net/fsPopup.asp?PosterID=604159&mode=posterInfo> Accessed April 8, 2026
14. Issa GC, Aldoss I, Thirman MJ, et al. Menin Inhibition With Revumenib for KMT2A-Rearranged Relapsed or Refractory Acute Leukemia (AUGMENT-101). *J Clin Oncol*. 2025;43(1):75-84.
15. Gordon SJV, Perner F, MacPherson L, et al. Catalytic Inhibition of KAT6/KAT7 Enhances the Efficacy and Overcomes Primary and Acquired Resistance to Menin Inhibitors in MLL Leukemia. *Cancer Discov*. 2025;15(10):2117-2138.

Figure Legends

Figure 1. Diagnostic workup of the patient's bone marrow sample. A) Morphology and Immunohistochemical (IHC) staining of diagnostic bone marrow. Upper: Wright-Giemsa staining captured at 20x and 50x magnification highlights blasts; **Lower:** IHC staining for MPO and NSE shows reactivity in blasts. **B) Identification of the novel *KAT6B::NUTM2B* fusion in the diagnostic bone marrow sample. Upper:** Schema of *KAT6B* (NM_012330) and *NUTM2B* (NM_001278495) gene structures as well as the cryptic deletion of approximately 4.8 Mb in relation to the formation of *KAT6B::NUTM2B* fusion, followed by partial sequence of the *KAT6B::NUTM2B* fusion transcript along with the predicted amino acid sequence. The transcript is an in-frame fusion of *KAT6B* exon 17 to *NUTM2B* exon 2 (mid-exon). **Lower:** Schematic diagrams of *KAT6B*, *NUTM2B* and the predicted *KAT6B::NUTM2B* chimeric proteins with functional domains. NEMM, N-terminal extension of MYST; PHD, plant homeodomain; MYST, histone acetyltransferase domain (HAT); Acidic domain, transcriptional activation and interaction with co-activators; SM, Serine-Methionine-rich region. **C) Global Gene Expression Profiling.** Global gene expression profiling was conducted using UMAP (Uniform Manifold Approximation and Projection) analysis as previously described (doi:10.1038/s41588-023-01640-3). The *KAT6B::NUTM2B*-positive case clustered with the *KAT6A-r* and *KMT2A-r* subtypes by UMAP. The UMAP plot was generated in the context of previously published pediatric AML cohort (n=887, doi:10.1038/s41588-023-01640-3) and cord blood CD34+ cells (n=5). **D) Normalized expression of *HOXA9* and *HOXA10* genes.** Expression levels are shown for the *KAT6B::NUTM2B*-positive patient along with reference cases from selected AML subtypes, including molecular categories known to be associated with *HOXA* activation (*KAT6A-r*, *KMT2A-r*, *NUP98-r* and *NPM1-mut*) and that do not have *HOXA* activation (*RUNX1::RUNX1T1* and *CBFB::MYH11*). The reference cases (n=374) were available from St. Jude Cloud (<https://www.stjude.cloud>) and included in a previously published pediatric AML study cohort

(doi:10.1038/s41588-023-01640-3). Expression values are shown as variance-stabilized counts (VST) derived from HTSeq counts as previously described⁷.

Figure 2. In vitro studies with *KAT6B::NUTM2B*-transduced murine bone marrow hematopoietic stem and progenitor cells (mHSPC). A) Schematic depiction of workflow.

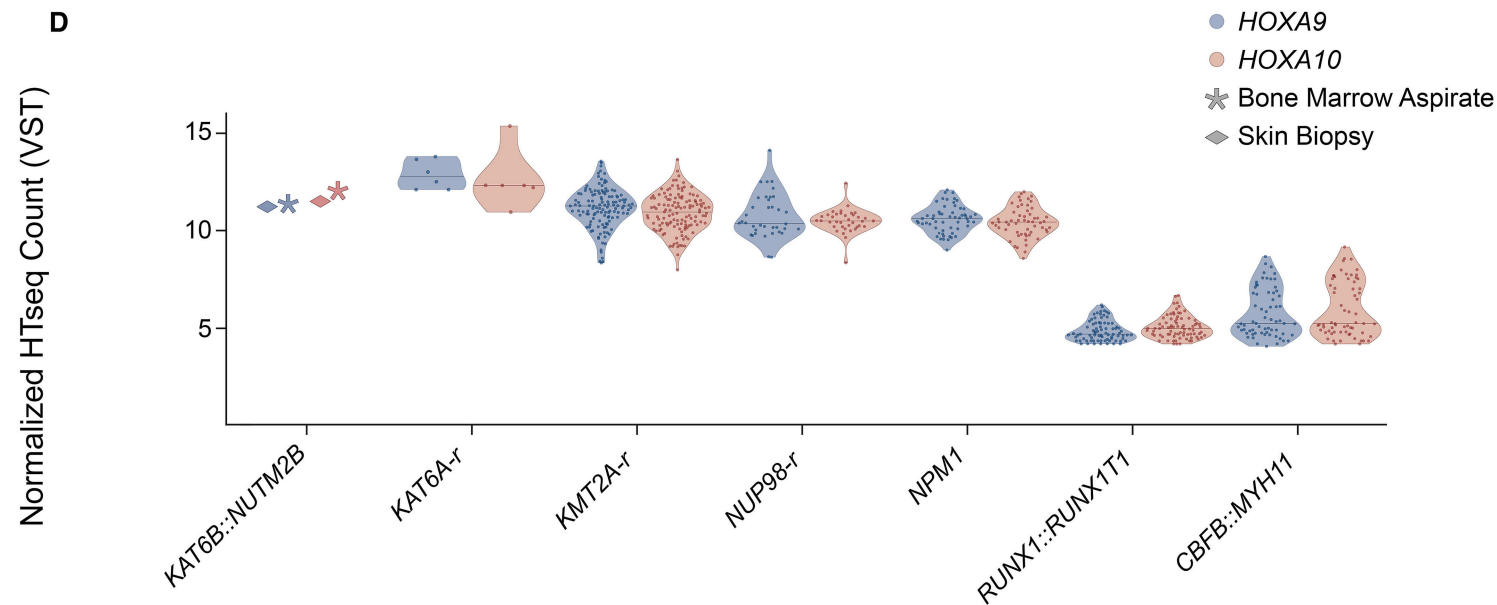
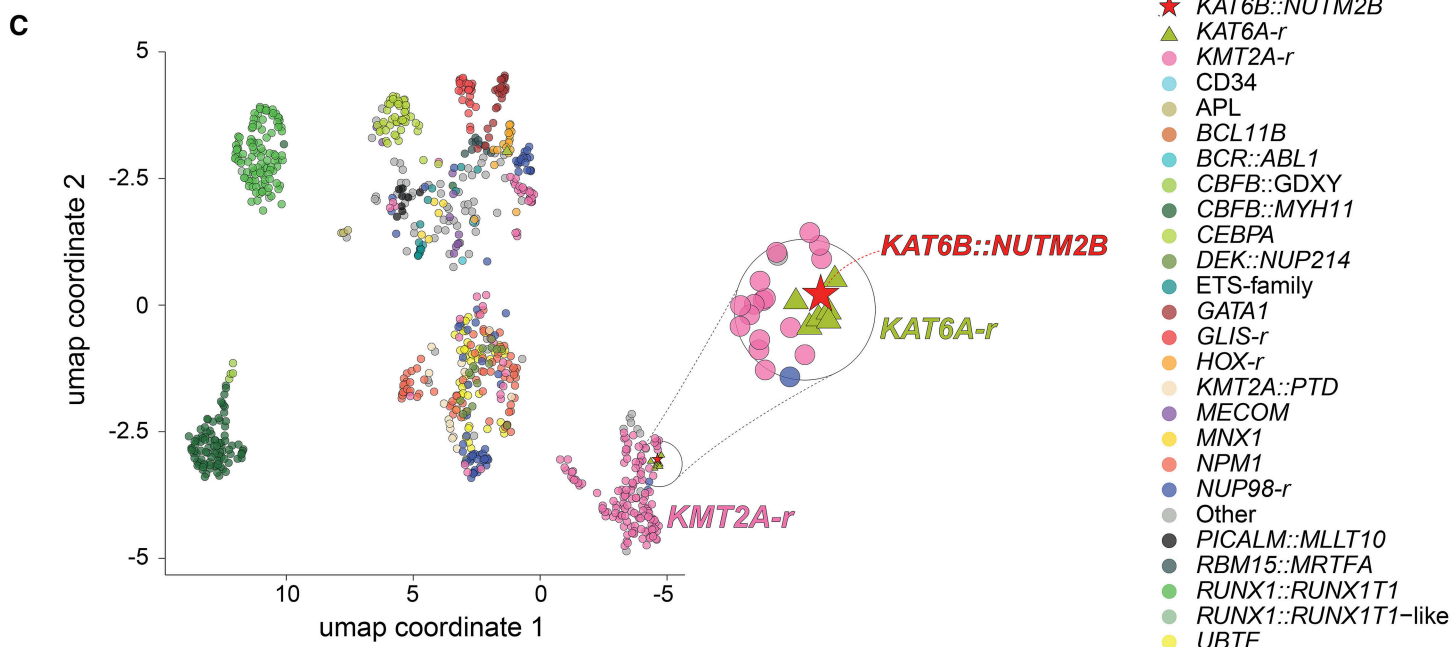
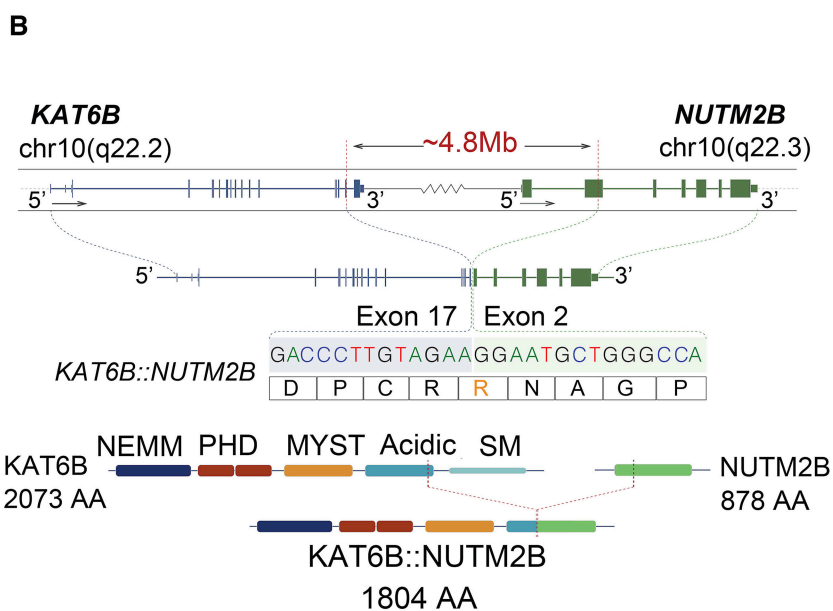
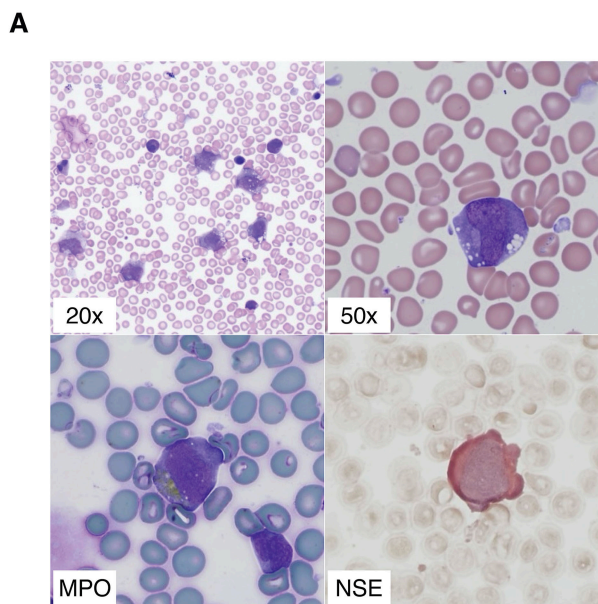
The GFP⁺-transduced cells were sorted and plated in methylcellulose for one week (W1). After this initial incubation, cells were divided as follows: (1) to continue colony-forming unit (CFU) assays without (I) and with (II) SNDX-5613 treatment, and (2) to assess the effects of SNDX-5613 treatment in liquid culture (III). **B) Colony forming unit (CFU) assay.** Transduced mHSPCs were plated in triplicate in methylcellulose (2×10^4 cells/35 mm dish). Colonies were counted and serially replated every 7 days. Results from one representative CFU assay are presented, with similar findings observed across multiple independent repeats. EV, empty vector. **C) Impact of SNDX-5613 treatment on colony formation in CFU assay.** Results are shown from a representative experiment (one of four independent replicates) conducted as outlined in Figure 2A-II.

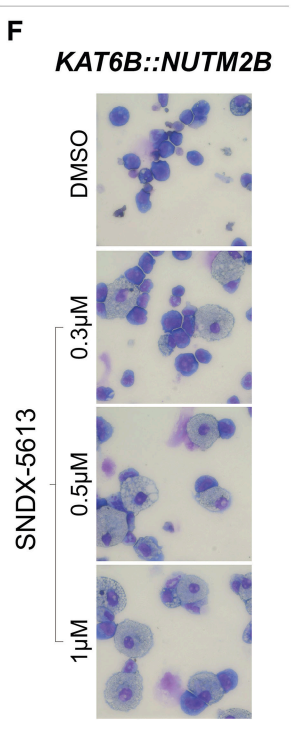
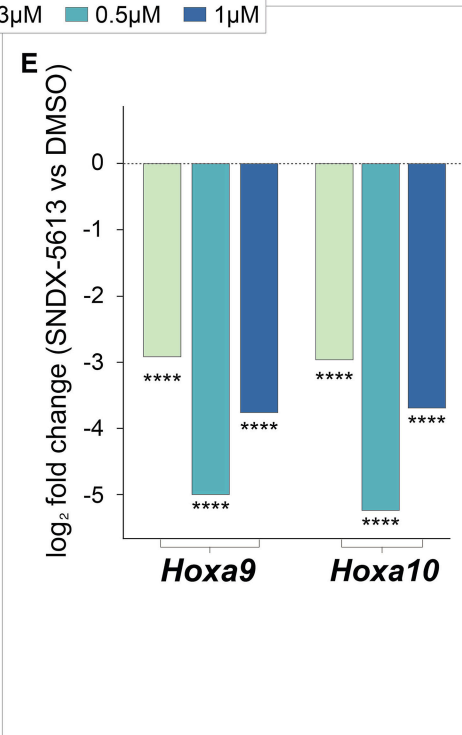
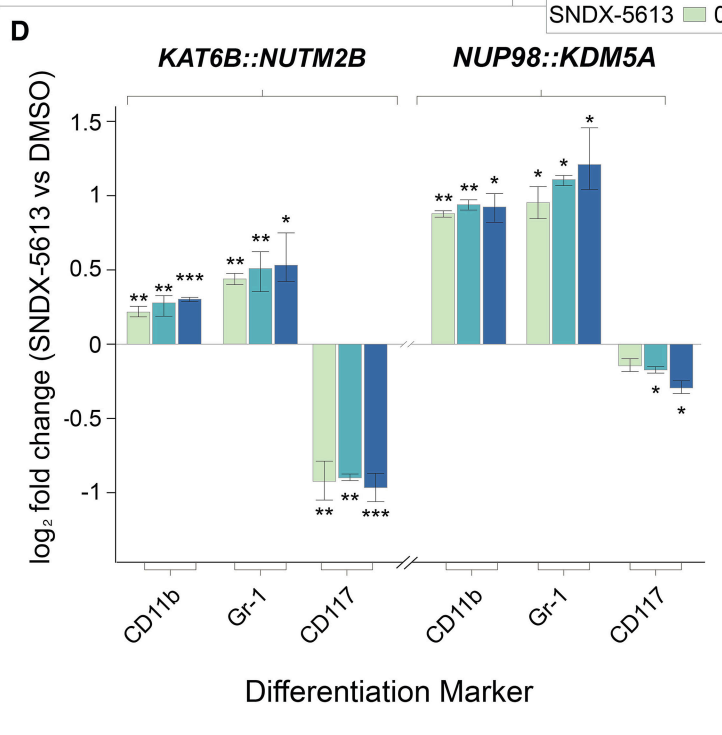
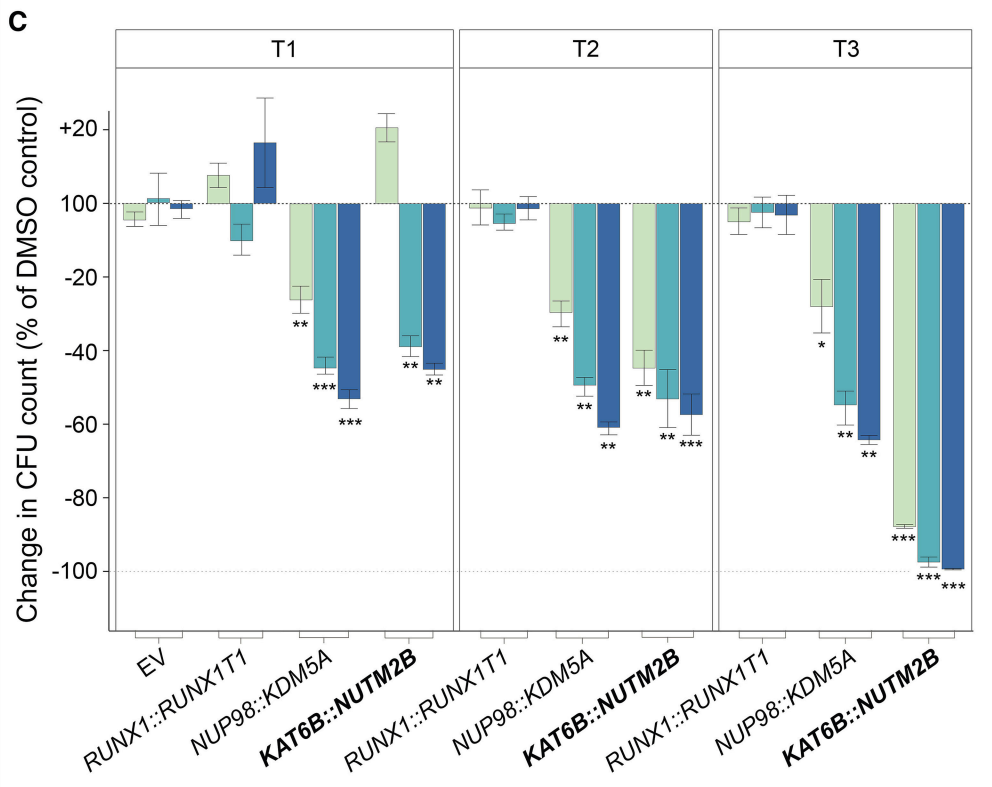
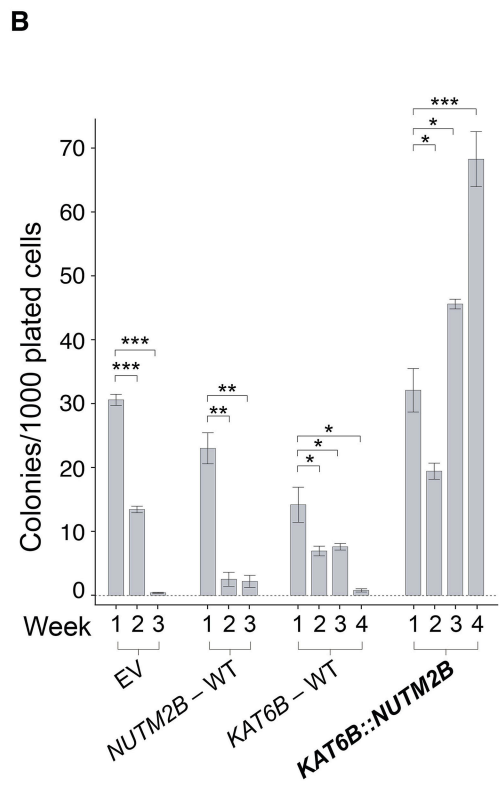
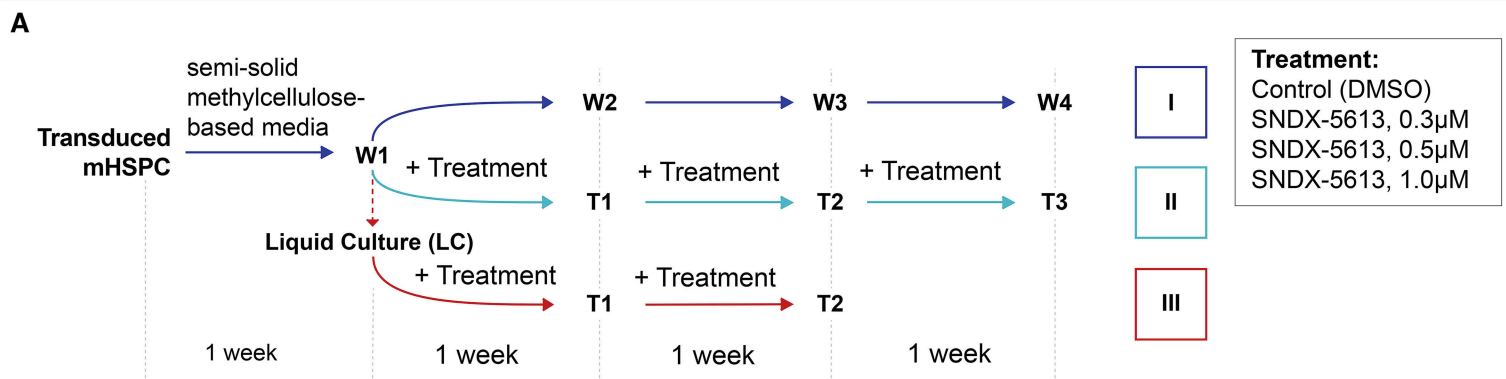
Transduced mHSPCs were plated in methylcellulose and treated with SNDX-5613 at 0.3 μ M, 0.5 μ M, 1.0 μ M, respectively, or with 0.1% DMSO (control). Treatment with the indicated concentrations of SNDX-5613 started after the initial one-week incubation in semi-solid culture. The process continued for 3 weeks, with cells replated and treated in fresh methylcellulose every 7 days. Colonies were counted prior to each replating. The x-axis shows time points after 1, 2, and 3 weeks of treatment (T1, T2, T3). The y-axis shows the relative change in colony-forming unit (CFU) counts compared to the DMSO control (% of DMSO control). Error bars represent standard deviation. Statistical significance was assessed using two-sided Welch's t-test. * $p < 0.05$; ** $p < 0.01$; *** $p < 0.001$. **D) Flow cytometry analysis of myeloid differentiation markers.**

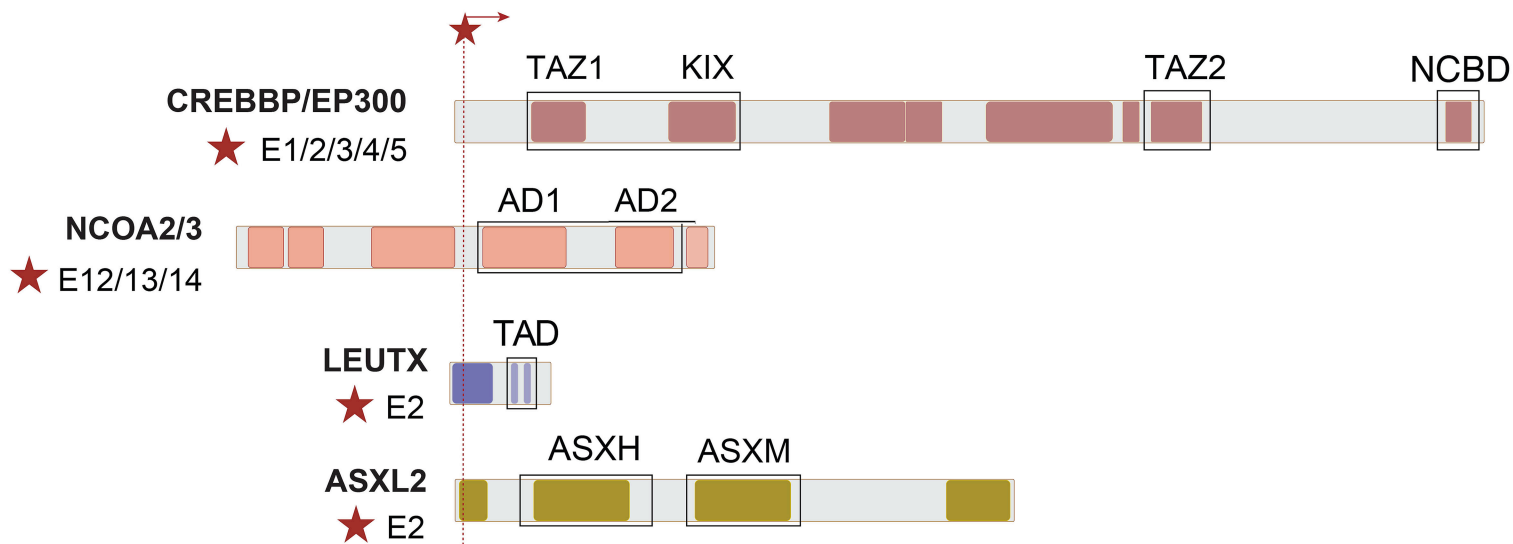
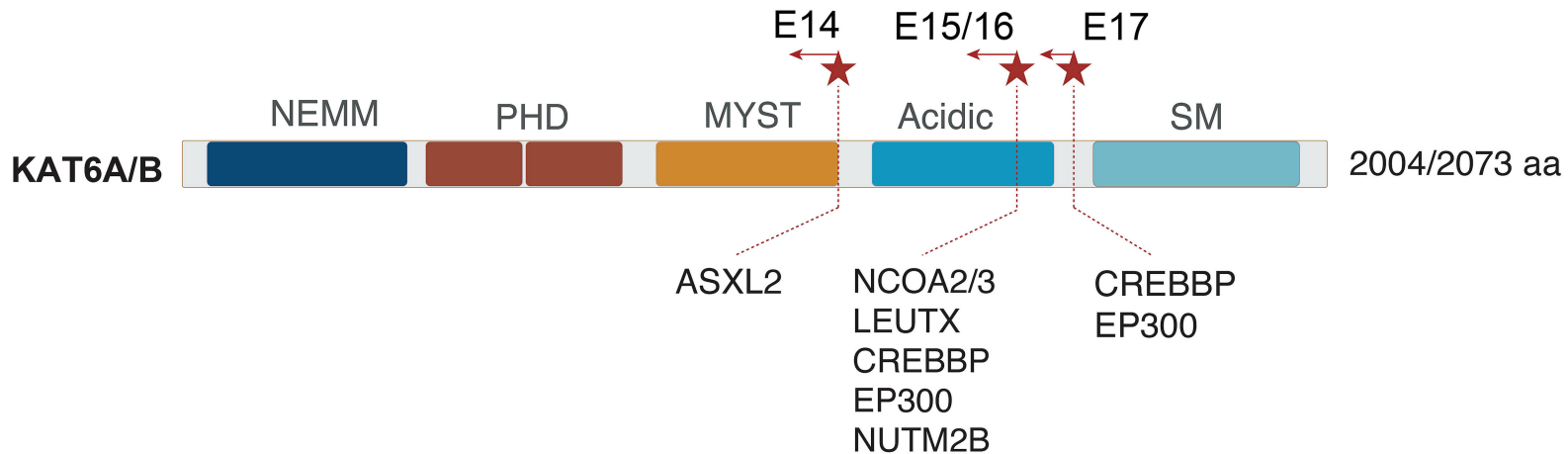
The mHSPCs transduced with *KAT6B::NUTM2B* and *NUP98::KDM5A*, respectively, were treated with SNDX-5613 at three concentrations or DMSO (control) in liquid culture (RPMI with cytokines) as outlined in figure 2A-III. Results from a representative experiment are depicted. Bar plots display the \log_2 fold change in mean fluorescence intensity (MFI) for CD11b, Gr-1 and CD117,

compared to their expression in transduced mHSPCs treated with DMSO control (SNDX-5613 vs. DMSO). Statistical significance was assessed using one-sided Welch's t-test based on the expected direction of change for each marker, * $p < 0.05$; ** $p < 0.01$; *** $p < 0.001$. **E) SNDX-5613 treatment reduced *Hoxa9* and *Hoxa10* expression at the transcriptional level.** The mRNA expression of *Hoxa9* and *Hoxa10* in *KAT6B::NUTM2B*-transduced mHSPCs were significantly downregulated by SNDX-5613 treatment compared with DMSO treatment (control). Cells in liquid culture were harvested after one and two weeks of treatment (T1 and T2, see Figure 2A-III), respectively; results are shown for T2. Bars represent \log_2 fold change (SNDX-5613 treated vs. DMSO) for *Hoxa9* and *Hoxa10*. Statistical significance was assessed using one-sided Welch's t-test (expected decrease). **** $p < 0.0001$. **F) Wright-Giemsa stained cytopins of *KAT6B::NUTM2B*-transduced cells** obtained from colony forming unit (CFU) assay harvested after one week of SNDX-5613 treatment (T1) as illustrated in Figure 2A-II.

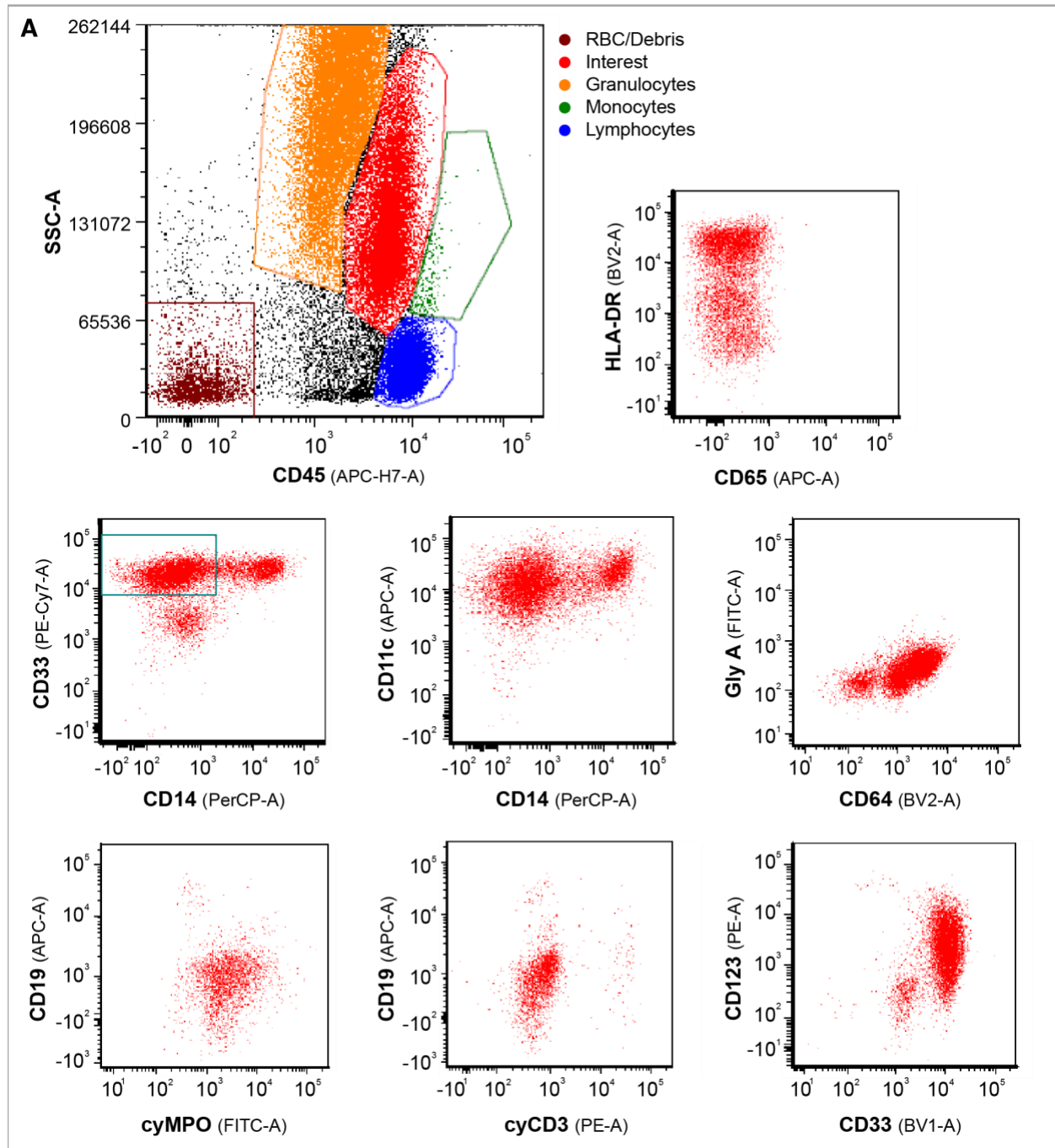
Figure 3. Schematic representation of KAT6A or KAT6B fusion proteins. Upper panel: KAT6A/B with known fusion junctions associated with different fusion partners. In all chimeric proteins, the N-terminal region of KAT6A/B is retained, including the MYST domain which mediates histone acetyltransferase (HAT) activity. **Lower panel:** C-terminal fusion partners to KAT6A and/or KAT6B reported in literature. Fusion junctions are indicated by red stars. Black boxes highlight retained transcriptional activation domains in all fusion partners. **Abbreviations:** E, exon; NEMM, N-terminal extension of MYST; PHD, plant homeodomain; MYST, histone acetyltransferase domain (HAT); SM, Serine-Methionine-rich region; TAZ1/2, Transcriptional adaptor Zinc-binding domain 1/2; KIX, CREB/Kinase Inducible Domain Interacting Domain; NCBD, Nuclear Coactivator Binding Domain; AD, activation domain; TAD, transactivation domain; ASXH, Asx Homology domain.



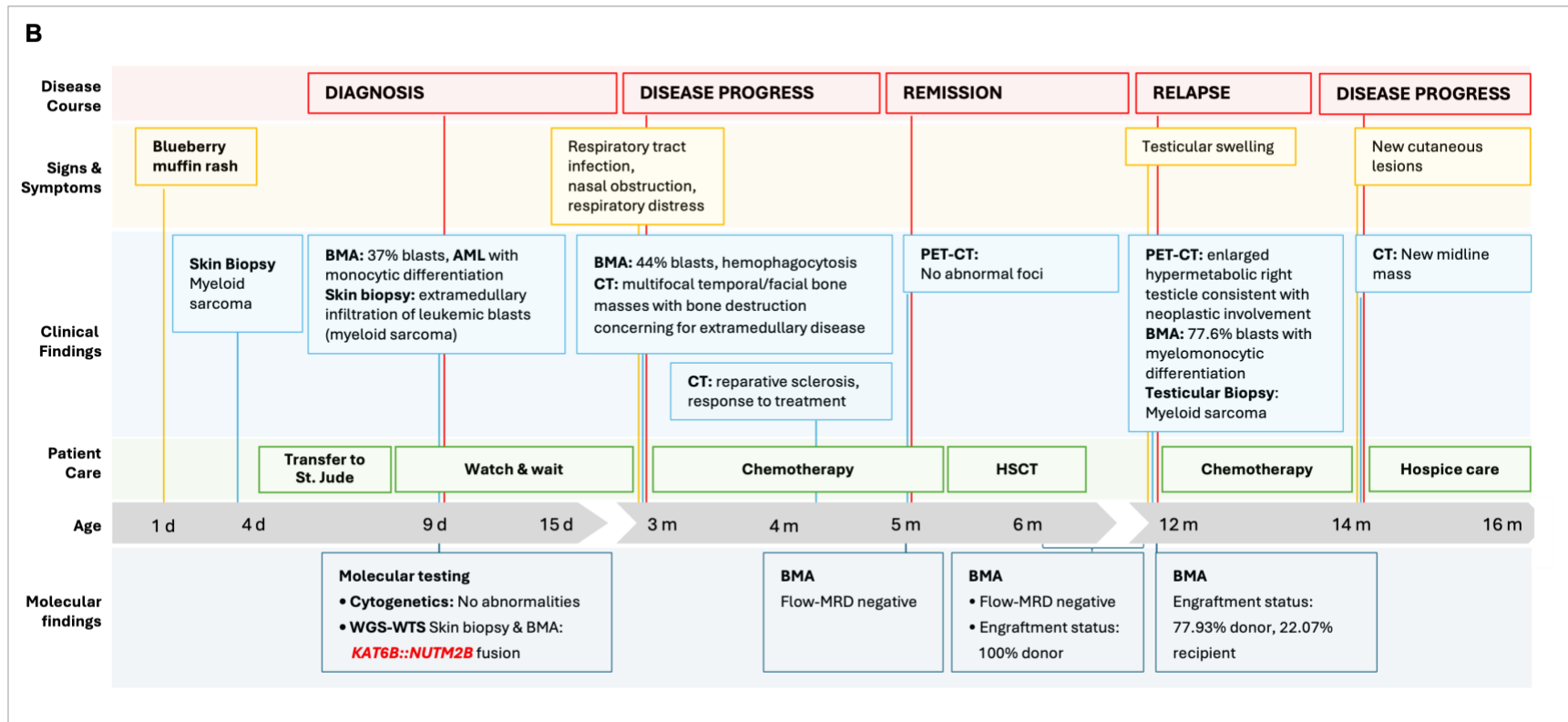




Supplementary Figure S1

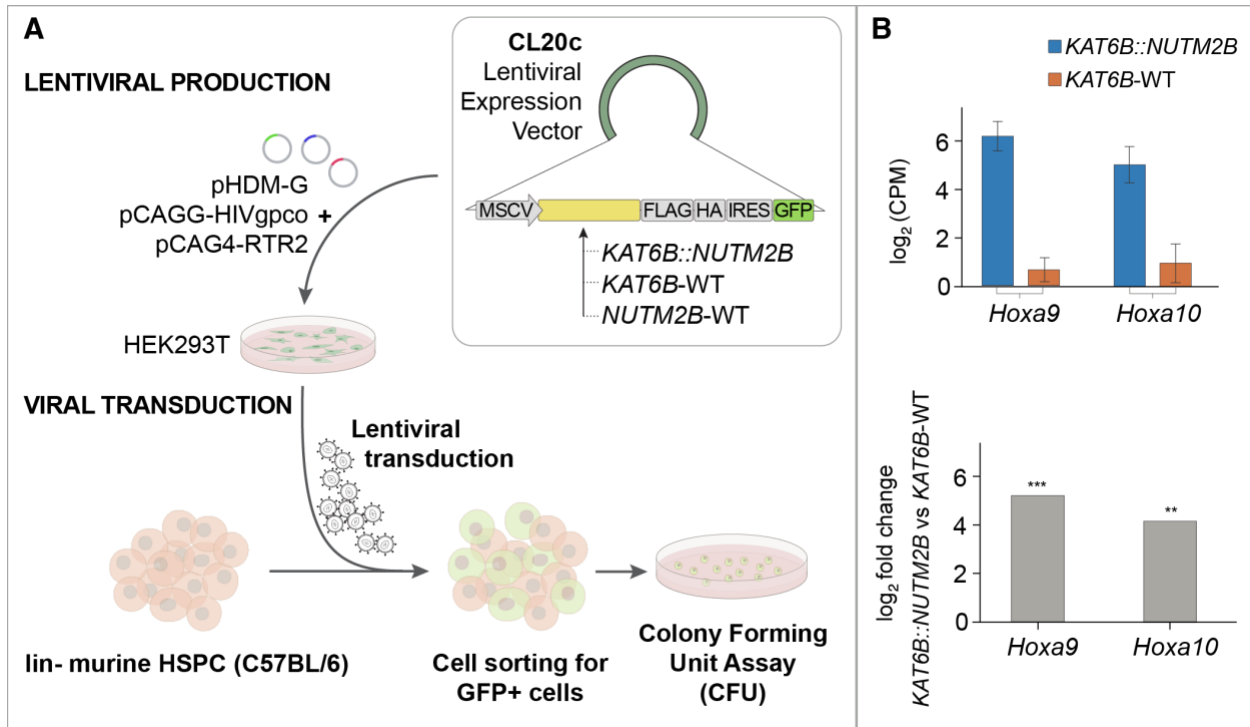


Supplementary Figure S1. Immunophenotypic characterization of patient's leukemia and the time course of the patient's disease. A) Immunophenotypic feature of the bone marrow aspirate sample collected at initial diagnostic work-up at St. Jude Children's Research Hospital. Expression of selected CD (cell differentiation) markers by flow cytometry analysis. Blasts are positive for monocytic markers CD64 and CD11c, but loss of CD14 expression is observed in the majority of blasts (green rectangle). Blasts are also positive for MPO, CD123 and HLA-DR, but negative for CD19 and cyCD3.



Supplementary Figure S1. B) The time course of the patient's disease since birth. Clinical signs and symptoms are shown in orange boxes, and pathology and imaging findings are shown in bright blue boxes. Patient management, including therapeutic interventions, is depicted in green boxes. Chemotherapy administered at disease progression consisted of Induction I (cytarabine, daunorubicin, etoposide and gemtuzumab) and Induction II (idarubicin and cytarabine), followed by haploidentical HSCT. At relapse, the patient received two cycles of azacitidine, gemtuzumab, and venetoclax. Molecular diagnostic results and disease monitoring are summarized at the bottom. **Abbreviations:** BMA, bone marrow aspirate; d/o, days old; HSCT, hematopoietic stem cell transplantation; m/o, months old; MRD, measurable residual disease; WGS, whole genome sequencing; WTS, whole transcriptome sequencing

Supplementary Figure S2



Supplementary Figure 2. In vitro cell model: Mouse hematopoietic stem and progenitor cells (mHSPCs) transduced with expression constructs, recapitulating *Hoxa9/10* dysregulation by *KAT6B::NUTM2B* fusion. A) Construction of wild-type *KAT6B* (*KAT6B-WT*), wild-type *NUTM2B* (*NUTM2B-WT*) and *KAT6B::NUTM2B* expression vectors and schematic of transduction and Colony Forming Unit (CFU) Assay. Coding sequences of human *KAT6B* (NM_012330), *NUTM2B* (NM_001278495) and *KAT6B::NUTM2B* fusion were synthesized and cloned into pENTR/D-TOPO Gateway entry vector (K240020, Thermo Fisher) by GenScript (Piscataway NJ) then transferred into MSCV-IRES-GFP (MPG) vector using Gateway LR clonase II enzyme system (Invitrogen, Waltham, MA, USA). For the generation of lentivirus, one million HEK293T cells were plated in each well of a 6-well plate for 24 h, then transiently co-transfected with lentiviral packaging helper plasmids pHDM-G, pCAGG-HIVgpc, pCAG4-RTR2 and the plasmid of interest at a 1:1 ratio. Transfections were carried out using either FuGene HD (Promega, Madison, WI, USA) or Lipofectamine (Thermo Fisher Scientific, Waltham, MA, USA) according to the manufacturer's instructions. After an incubation period of 48 h, the supernatant containing the lentivirus was collected for transduction of mice hematopoietic stem and progenitor cells (mHSPCs) isolated from bone marrow sample obtained from C57BL/6 mice (EastSep™ Mouse Hematopoietic Progenitor Cell Isolation Kit, STEMCELL TECHNOLOGIES™) followed by colony forming unit (CFU) assay. B) *Hoxa9* and *Hoxa10* expression at the

transcriptional level. Upper: Expression levels of *Hoxa9* and *Hoxa10* in *KAT6B::NUTM2B* and *KAT6B*-WT transduced mHSPCs; Lower: Relative expression of *Hoxa9* and *Hoxa10* in *KAT6B::NUTM2B* transduced mHSPCs compared to *KAT6B*-WT transduced cells (*KAT6B::NUTM2B* vs. *KAT6B*-WT). *** $p < 0.001$, ** $p < 0.01$.

Supplementary Table S1. Summary of reported cases with *KAT6A/B* fusions in infant AML/myeloid sarcoma and additional cases with other *KAT6A* or *KAT6B* fusion partners not observed in infant patients.

Fusion partner	No. of cases	Age at DX	Diagnosis	BM-Blast	FAB classification	Karyotype	Clinical signs & symptoms	Clinical course	Reference
<i>KAT6A::CREBBP</i>	26*	median ~1 month (1 day-12 months) *	AML, myeloid sarcoma	52% (med.)	M4, M5	See original publication	Cutaneous lesions in 82%, disseminated intravascular coagulation in 30% and erythrophagocytosis in 50% of infants for whom data was available	7 of 26 cases with spontaneous remission, 4 of whom relapsed	Coenen et al., <i>Blood</i> (2013)
<i>KAT6A::CREBBP</i>	1**	<1 month	Myeloid sarcoma	NA	M4	NA	Cutaneous lesions, hemophagocytosis, hepatosplenomegaly	Deceased	Francianne Gomes Andrade et al., <i>Revista Brasileira de Hematologia e Hemoterapia</i> (2016)
<i>KAT6A::CREBBP</i>	1	<1 month	Myeloid sarcoma + BM involvement	35%	M4	46,XX (fusion identified by FISH)	Cutaneous lesions, hepatosplenomegaly	Spontaneous remission after 5 months	Barrett R, et al. <i>Pediatr Blood Cancer</i> . (2017)
<i>KAT6A::EP300</i>	1	Newborn	Myeloid sarcoma, AML	44%	M5b	46,XX,t(8;12;22)(p11.2;q24.1;q13)[15]/46,XX[5]	Cutaneous lesions	Spontaneous remission within 3 months	Ikawa, Y., et al <i>Leukemia & Lymphoma</i> (2018).
<i>KAT6A::EP300</i>	1	1 month	Myeloid sarcoma	NA	NA	NA	Cutaneous lesions	Spontaneous remission	Hosahalli Vasanna, et al. <i>Medicine</i> (2023)
<i>KAT6A::NCOA2</i>	1	7 months	Myeloid sarcoma, AML	46%	M4/5	46,XX,t(1;20)(q21;q21.3),-8,der(21)t(1;21)(q21;q22),+mar[16]/46,XX,idem,add(6)(q27)[4]	Cutaneous lesions (scalp)	Relapse pre HSCT, death 5 months after diagnosis	Koduru, Prasad R, et al. <i>Journal of Pediatric Hematology/Oncology</i> (2017)
<i>KAT6A::LEUTX</i>	1	2 weeks	Myeloid sarcoma, AML	37.2%	M4/5	NA	Cutaneous lesions, hepatosplenomegaly, thrombocytopenia, leukocytosis	Death within 5 days of diagnosis under chemotherapy, leukemic infiltration of lung and heart	Sramkova, L, et al., <i>Pediatr Blood Cancer</i> (2020)
<i>KAT6A::LEUTX</i>	1	3 months	Myeloid sarcoma, AML	26%	M4	46,XX,t(8;19)(p11.2;q13.3)[16]/46,XX [4]	Cutaneous lesions, hepatosplenomegaly, thrombocytopenia, leukocytosis	Remission after chemotherapy	Eason, Ashley C., et al. <i>Case Reports in Hematology</i> (2019)

KAT6A::LEUTX	1	8 months	AML	72%	M5a	46,XY,t(8;19)(p11;q13.2)[8]/46,XY,t(8;19),1,+1q[22]/46,XY,t(8;19),-16,+16q+[6]	Hepatosplenomegaly, enlarged lymph nodes, disseminated intravascular coagulation, erythrophagocytosis	Death after bone marrow transplantation due to veno-occlusive disease	<i>A. Brizard et al., Leukemia Research (1988)</i>
KAT6A::ASXL2	1	6 years	tMDS	5%	NA	46,XY,del(8)(p21)[17]/46,XY[3]	NA	Initial diagnosis: AML M2 with t(8;21)(q22;q22)/ <i>RUNX1::RUNX1T1</i> at age 4; relapsed at age 5 (<i>RUNX1::RUNX1T1</i>); developed hypocellular dysplasia at age 6 with new t(2;8)(p23;p11.2)/ <i>KAT6A::ASXL2</i> and persistent <i>RUNX1::RUNX1T1</i> ; died of infectious complications	<i>Imamura et al., Genes Chromosom. Cancer (2003)</i>
KAT6A::NCOA3	1	75 years	AML	91%	M5	46,XX,t(8;20)(p11;q13)[23]	Splenomegaly, disseminated intravascular coagulation.	Treatment with hydroxyurea + low dose cytosine arabinoside, no remission achieved and patient passed from intracerebral hemorrhage within 3 months of diagnosis	<i>Murati et al., British Journal of Hematology (2004)</i>
KAT6B::CREBBP	1	4 years	AML	94%	M5a	47,XX,der(7)t(7;10)(p13;p11),+8,der(10)t(7;10)(p13;p11)t(10;16)(q22;p13),der(16)t(10;16)(q22;p13)[19]/46,XX[6]	NA	Patient treated according to NOPHO-93	<i>Panagopoulos I. et al., Hum Mol Genet. (2001)</i>
KAT6B::CREBBP	1	52 years	tMDS	1.8%	NA	46,XX,t(10;16)(q22;p13)[18]/46,XX[2]	NA	History of AML-M1, 95% BM blasts, normal Karyotype, treated with intensive chemotherapy ~1.5years prior to diagnosis of tMDS. Treatment of tMDS: Supportive management, progress to 21% blasts after 9 months, no monocytic differentiation	<i>Kojima K. et al. British Journal of Haematology (2003)</i>
KAT6B::CREBBP	1	84 years	AML	89%	M5b	46,XY,t(10;16)(q22;p13)	NA	no curative therapy, death one month after diagnosis	<i>Vizmanos, J.L. et al. Genes Chromosom. Cancer (2003)</i>
KAT6B::CREBBP	1	NA	AML	NA	M4	46,XX,t(10;16)(q21;p13),t(11;17)(q23;q21)	NA		<i>Murati, A. et al. British Journal of Haematology (2004)</i>

* Twenty-six of 62 cases in this study cohort were congenital/infant AML (case IDs: 3, 4, 16, 17, 19, 21, 23, 28, 29, 34, 35, 37, 38, 40, 41, 43, 46, 47, 48, 51, 52, 55, 59, 60, 61, 62)

** One of 5 cases in this study cohort showed *KAT6A::CREBBP*